Functional and structural correlations of individual αIIbβ3 molecules

Rustem I. Litvinov, Chandrasekaran Nagaswami, Gaston Vilaire, Henry Shuman, Joel S. Bennett, and John W. Weisel

The divalent cation Mn^{2+} and the reducing agent dithiothreitol directly shift integrins from their inactive to their active states. We used transmission electron microscopy and laser tweezers–based force spectroscopy to determine whether structural rearrangements induced by these agents in the integrin αIIbβ3 correlate with its ability to bind fibrinogen. Mn^{2+} increased the probability of specific fibrinogen-αIIbβ3 interactions nearly 20-fold in platelets, and both Mn^{2+} and dithiothreitol increased the probability more than 2-fold using purified proteins. Of 3 αIIbβ3 conformations, closed with stalks touching, open with stalks separated, and globular without visible stalks, Mn^{2+} and dithiothreitol induced a significant increase in the proportion of open structures, as well as structural changes in the αIIbβ3 headpiece. Mn^{2+} also increased the number of complexes between fibrinogen and purified αIIbβ3 molecules, all of which were in the open conformation. Finally, Mn^{2+} induced the formation of αIIbβ3 clusters that resulted from interactions exclusively involving the distal ends of the stalks. These results indicate that there is a direct correlation between αIIbβ3 activation and the overall conformation of the molecule. Further, they are consistent with the presence of a linked equilibrium between single inactive and single active αIIbβ3 molecules and active αIIbβ3 clusters. (Blood. 2004;104: 3979-3985)

Introduction

The activity of circulating platelets is tightly regulated to prevent the spontaneous formation of platelet aggregates.[1] Thus, circulating platelets are inactive until they adhere to exposed subendothelial matrix or are stimulated by soluble agonists such as adenosine diphosphate (ADP) and thrombin. Each activating event is associated with a change in platelet shape, reorganization of the platelet cytoskeleton, secretion of platelet granules, and an increase in the affinity of the integrin αIIbβ3 for soluble ligands such as fibrinogen and von Willebrand factor. The latter is responsible for platelet aggregation when the macromolecular ligands bind to activated αIIbβ3 and bridge adjacent platelets.[2]

Although the activation state of αIIbβ3 is normally regulated by agonist-generated "inside-out" signaling,[1] αIIbβ3 can also be activated experimentally by perturbing the conformation of its extracellular domain using Mn^{2+} ions[3,4] or the reducing agent dithiothreitol (DTT).[5,6] Thus, in platelets, Mn^{2+} has been reported to activate αvβ3 and αIIbβ3, thereby promoting their interaction with ligands such as fibrinogen, von Willebrand factor, vitronectin, and osteopontin, mimicking the consequences of conventional inside-out signaling.[3,4] Mn^{2+} also stabilizes platelet-fibrinogen interactions.[7] Moreover, in experiments using purified integrins, Mn^{2+} affects the binding kinetics, affinity, and specificity toward synthetic and natural ligands.[8-11] Mn^{2+}-induced changes in integrin function have been attributed to specific conformational rearrangements in the integrin ectodomain,[12] a suggestion supported by electron microscope studies showing that Mn^{2+} promotes the opening of integrin molecules into extended structures.[13-15]

Millimolar concentrations of DTT also induce platelet aggregation by directly stimulating ligand binding to αIIbβ3.[5,6] How DTT activates αIIbβ3 is unclear. β3 has been reported to contain an extracellular redox site that is associated with the presence of 2 unpaired cysteines in inactive αIIbβ3 and 6 unpaired cysteines following exposure of αIIbβ3 to DTT.[16] However, the identity of the putatively unpaired cysteines in either inactive or active forms of αIIbβ3 has not been determined, and it has been proposed that αIIbβ3 activation by DTT may involve disulfide bond rearrangement of the originally unpaired cysteines, as well as overall bond reduction.[16,17]

The ability of Mn^{2+} and DTT to enhance integrin function, as well as perturb the conformation of integrin ectodomains, provides an opportunity to test the hypothesis that there is an equilibrium between inactive and active integrin activation states that is a consequence of a reversible structural rearrangement of the entire integrin molecule. To address this hypothesis, we used transmission electron microscopy to probe for structural differences between αIIbβ3 in the presence of Ca^{2+}, Mn^{2+}, and DTT and laser tweezers–based force spectroscopy to measure the fibrinogen-binding function of the integrin in the presence of each at the single molecule level. We found that both Mn^{2+} and DTT increase the probability of specific interactions between αIIbβ3 and fibrinogen, but they do so without changing the average yield strength of fibrinogen binding. Both agents also induce a change in the shape of the αIIbβ3 headpiece, shift αIIbβ3 from a closed conformation with stalks touching to an open conformation with stalks separated, and stimulate the formation of clusters of the open αIIbβ3

From the Department of Cell and Developmental Biology, University of Pennsylvania School of Medicine, Philadelphia; the Department of Physiology, University of Pennsylvania School of Medicine, Philadelphia; and the Hematology-Oncology Division of the Department of Medicine, University of Pennsylvania School of Medicine, Philadelphia.

Submitted April 16, 2004; accepted August 4, 2004. Prepublished online as *Blood* First Edition Paper, August 19, 2004; DOI 10.1182/blood-2004-04-1411.

Supported by the National Institutes of Health (grants HL57407, HL30954, HL40387, and HL62250).

Reprints: John W. Weisel, Department of Cell and Developmental Biology, University of Pennsylvania School of Medicine, 421 Curie Blvd, 1054 BRB II/III, Philadelphia, PA 19104-6058; e-mail: weisel@mail.med.upenn.edu.

The publication costs of this article were defrayed in part by page charge payment. Therefore, and solely to indicate this fact, this article is hereby marked "advertisement" in accordance with 18 U.S.C. section 1734.

conformer. These results indicate that there is a direct correlation between the activation of αIIbβ3 and the overall conformation of the molecule. Further, they are consistent with the presence of a linked equilibrium between inactive and active αIIbβ3 molecules and αIIbβ3 clusters.

Materials and methods

Laser tweezers measurements

Using laser tweezers to measure integrin function on platelets has been described previously in detail.[18] Briefly, we used a custom-built laser tweezers setup assembled from a Nikon Diaphot 300 inverted microscope (Nikon, Mellville, NY), 100 × 1.3NA Fluor lens and a Spectra-Physics (Mountain View, CA) FCBar Nd:YAG laser to measure the strength of fibrinogen binding to human platelets or purified αIIbβ3 in the presence of either Ca^{2+} or Mn^{2+}. For these measurements, human fibrinogen (American Diagnostica, Stamford, CT) was covalently bound to 0.93 μm carboxylate-modified latex beads using N-(3-dimethylaminopropyl)-N′-ethylcarbodiimide hydrochloride as a cross-linking agent in a 2-step procedure described in the TechNote no. 205 issued by Bangs Laboratories (Fishers, IN). Before use, the fibrinogen-coated beads were disaggregated by mild sonication and used at a concentration of approximately 10^7/mL. For studies using purified human αIIβ3, the purified integrin (Enzyme Research Laboratories, South Bend, IN) at a concentration of 1 mg/mL in 0.01 M *N*-2-hydroxyethylpiperazine-*N*′-2-ethanesulfonic acid (HEPES) buffer, pH 7.4, containing 60 mM octyl-glucoside was bound covalently to polyacrylamide-coated 1.40 μm silica pedestals using glutaraldehyde as previously described.[18] Prior to immobilization, the αIIbβ3 was preincubated with either 1 mM $CaCl_2$, 1 mM $MnCl_2$, or 5 mM DTT/1 mM $CaCl_2$ in the same binding buffer at 37°C for 30 minutes. Interactions between fibrinogen and purified αIIbβ3 were studied in 0.1 M HEPES buffer, pH 7.4, containing 2 mg/mL bovine serum albumin, 0.1% Triton X-100, and either 1 mM $CaCl_2$, 1 mM $MnCl_2$, or 5 mM DTT/1 mM $CaCl_2$. To measure fibrinogen binding to αIIbβ3 on living platelets, an individual platelet was trapped from a suspension of gel-filtered human platelets containing approximately 5 × 10^6 platelets/mL and approximately 10^5/mL fibrinogen-coated beads and manually attached to a 5-μm diameter silica pedestal coated with polylysine.[18] All experiments with unstimulated platelets were performed in a 4 mM HEPES gel-filtration buffer, pH 7.4, containing 135 mM NaCl, 2.7 mM KCl, 5.6 mM glucose, 1 mM $CaCl_2$, 3.3 mM NaH_2PO_4, and 0.35 mg/mL bovine serum albumin.

To measure the rupture force between fibrinogen and either purified αIIbβ3 or αIIbβ3 on platelets, a fibrinogen-coated bead, trapped by the laser light, was brought to a distance of 2 to 3 μm from the αIIbβ3-coated pedestal or immobilized platelet. After oscillation of the bead was initiated at 5 Hz or 50 Hz with 0.8 μm peak-to-peak amplitude, the bead was brought into contact with the platelet or the pedestal by micromanipulation using a keyboard-controlled piezoelectric stage. Data collection was initiated at the first contact between the bead and the platelet or pedestal. Rupture forces following repeated contacts between the platelet or the pedestal and the bead were collected for periods of several seconds to 1 minute and were displayed as normalized force histograms for each experimental condition. Because only a small percentage of contact/detachment cycles result in effective receptor-ligand binding/unbinding, data from 10 to 22 experiments, representing 3 × 10^3 to 10^5 individual measurements, were combined. Individual forces measured during each contact-detachment cycle were collected into 10 pN-wide bins. The number of events in each bin was plotted against the average force for that bin after normalizing for the total number of interaction cycles. The percentage of events in a particular force range (bin) represents the probability of rupture events at that tension. Optical artifacts observed with or without trapped latex beads produce signals that appeared as forces below 10 pN.[18] Accordingly, rupture forces in this range were not considered when these data were analyzed.

Transmission electron microscopy

Rotary-shadowed samples were prepared using a modification of standard procedures[19,20] by spraying a dilute solution of molecules in a volatile buffer (0.05 M ammonium formate) and glycerol (30%-50%) onto freshly cleaved mica and shadowing with tungsten in a vacuum evaporator (Denton Vacuum, Cherry Hill, NJ).[21] All specimens were examined in a FEI/Philips 400 electron microscope (Philips Electronic Instruments, Mahwah, NJ), operating at 80 kV and at a magnification of × 60 000. The molecular dimensions for approximately 100 individual images from the various groups of αIIbβ3 molecules were measured after scanning negative prints using Adobe Photoshop 7.0.1. Measurements were made with a Photoshop tool calibrated to have 1.6 nm resolution. Molecular dimensions of the digitized images were corrected for a shell of tungsten by subtracting 1 nm on each side of a measured molecule.

Results

Interaction of Mn^{2+}-treated platelets with fibrinogen

When probed by laser tweezers–based force spectroscopy, the vast majority of the interactions between surface-bound fibrinogen and unstimulated platelets in the presence of Ca^{2+} were characterized by rupture forces that ranged from 10 pN to several tens of pN. Moreover, the probability of detecting these rupture forces decreased exponentially as the rupture force increased (Figure 1A). However, the same platelets incubated with 1 mM $MnCl_2$ for 5 minutes at 25°C were highly reactive with fibrinogen-coated beads, producing a peak in the histogram of rupture forces that ranged from 60 to 110 pN (Figure 1B). Thus, the cumulative probability of detecting rupture forces greater than 60 pN, which we previously found to be specific for fibrinogen binding to αIIbβ3,[18] increased nearly 20-fold. To confirm that the Mn^{2+}-induced peak of rupture forces resulted from fibrinogen binding to αIIbβ3, measurements were repeated in the presence of either of the αIIbβ3 antagonists, tirofiban, or abciximab.[18] As shown in Figure 1C-D, each antagonist abrogated the effect of Mn^{2+} and returned the force histograms to that of unstimulated platelets incubated with Ca^{2+}.

Interaction of Mn^{2+}-treated αIIbβ3 preparations with fibrinogen

To verify that the increase in rupture force we observed between platelets and fibrinogen-coated beads in the presence of Mn^{2+} resulted from an increase in the affinity of individual αIIbβ3 molecules and was independent of possible Mn^{2+}-induced changes in the platelet membrane, we measured rupture forces between fibrinogen-coated beads and purified αIIbβ3 that had been preincubated with 1 mM Mn^{2+} or 1 mM Ca^{2+}. Consistent with our

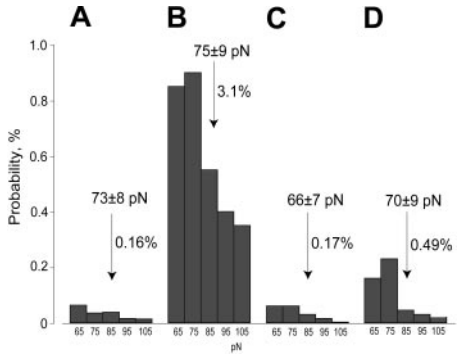

Figure 1. Force distribution histograms of fibrinogen binding to Mn^{2+}-activated platelets as measured using laser tweezers. The histograms represent rupture forces greater than 60 pN, previously shown to be specific fibrinogen binding to αIIbβ3.[18] The average yield strength in pN and the cumulative probability of specific fibrinogen binding (%) for each histogram are also shown. (A) Unstimulated platelets. (B) Platelets incubated with 1 mM Mn^{2+} for 5 minutes at 25°C. (C) Platelets incubated with 1 mM Mn^{2+} in the presence of 20 μM tirofiban. (D) Platelets incubated with 1 mM Mn^{2+} in the presence of 100 μg/mL abciximab.

previously reported laser tweezers measurements using purified αIIbβ3,[18] we found that the cumulative probability of detecting rupture forces greater than 60 pN was 2.1% in the presence of 1 mM Ca^{2+}, indicating that some of the purified αIIbβ3 was in an active conformation (Figure 2A). Others have observed that approximately 10% of the αIIbβ3 isolated from platelets is in an active conformation.[22] Nonetheless, as shown in Figure 2B, the Mn^{2+}-treated preparations were much more reactive with fibrinogen-coated surfaces, such that the cumulative probability of detecting rupture forces greater than 60 pN increased to 4.5%. The ability of the αIIbβ3 antagonists tirofiban and abciximab to decrease this probability to 0.4% confirmed that rupture forces greater than 60 pN resulted from fibrinogen bound to αIIbβ3 (Figure 2C-D). It is noteworthy that, despite the presence of Mn^{2+}, the yield strength of αIIbβ3-fibrinogen binding was not changed substantially, whereas the cumulative probability of specific rupture forces greater than 60 pN increased more than 2-fold. Thus, these results are consistent with the hypothesis that Mn^{2+} binding directly induces an increase in the affinity of individual αIIbβ3 molecules for fibrinogen.

Mn^{2+}-induced changes in the conformation of αIIbβ3

Purified αIIbβ3 molecules from the same preparation used for the laser tweezers experiments were visualized by transmission electron microscopy after rotary shadowing with tungsten. Previous electron microscopy studies indicated that αIIbβ3 molecules are composed of a dense "headpiece" and 2 "stalks," one from each subunit of the heterodimer.[23] The headpiece, composed of the amino-terminal portions of the extracellular domains of αIIb and β3, contains the ligand-binding site of the integrin, whereas the stalks contain the transmembrane and cytoplasmic domains of each subunit. From the observations of more than 2000 individual images, we were able to distribute αIIbβ3 molecules into 3 groups. Group 1 consists of relatively compact molecules in which the stalks appear to touch ("closed" images) (Figure 3A). Group 2 consists of extended molecules in which the stalks are separated ("open" images) (Figure 3B). Group 3 consists of globular heads in which the stalks are not visualized.

Although each group was present regardless whether αIIbβ3 had been incubated with Ca^{2+} or Mn^{2+}, the distribution was significantly different. As shown in Table 1, there was a large increase in the proportion of open (group 2) structures in the presence of Mn^{2+} (60% ± 4% in the presence of 1 mM Mn^{2+} versus 11% ± 4% in presence of Ca^{2+}, $P < .001$), with corresponding decreases in the proportion of group 1 (24% ± 3% in the presence of 1 mM Mn^{2+} versus 51% ± 12% in the presence of Ca^{2+}, $P < .001$) and group 3 structures (17% ± 3% in the presence of 1 mM Mn^{2+} versus 38% ± 10% in presence of Ca^{2+}, $P < .001$).

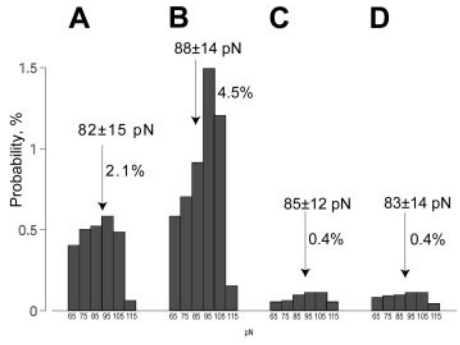

Figure 2. Force distribution histograms of fibrinogen binding to purified surface-bound αIIbβ3 preincubated with Ca^{2+} or Mn^{2+}. In the experiments shown, fibrinogen-coated beads were oscillated at 5 Hz touching the αIIbβ3-coated pedestals repeatedly. These data represent rupture forces greater than 60 pN, indicative of specific fibrinogen binding to αIIbβ3.[18] The average yield strength in pN and the cumulative probability of specific fibrinogen binding (%) for each histogram are also shown. (A) Fibrinogen binding to αIIbβ3 immobilized in the presence of 1 mM Ca^{2+}. (B) Fibrinogen binding to αIIbβ3 immobilized in the presence of 1 mM Mn^{2+}. (C) Fibrinogen binding to αIIbβ3 treated with 1 mM Mn^{2+} measured in the presence of 50 μM tirofiban. (D) Fibrinogen binding to αIIbβ3 treated with 1 mM Mn^{2+} measured in the presence of 100 μg/mL abciximab.

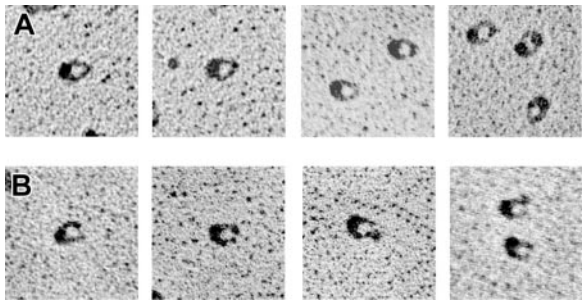

Figure 3. Transmission electron microscopy of purified αIIbβ3 in the presence of 1 mM Ca^{2+} or 1 mM Mn^{2+}. Individual αIIbβ3 molecules were visualized using transmission electron microscopy after rotary shadowing with tungsten. The images could by classified into 3 groups, of which 2 are shown. (A) Closed structures with the tips of the αIIb and β3 stalks touching that were obtained in the presence of 1 mM Ca^{2+}. (B) Open structures with the αIIb and β3 stalks separated that were obtained in the presence of 1 mM Mn^{2+}. A minority of structures consisting of globular headpieces with no visible stalks were also observed in the presences of both Ca^{2+} and Mn^{2+}. Magnification, × 170 000.

We also compared the molecular dimensions of individual αIIbβ3 molecules in the presence of Ca^{2+} or Mn^{2+} using digitized images of the electron micrographs. In the presence of Ca^{2+}, there were no significant differences in the dimensions of the αIIbβ3 headpiece when the molecules were in either the open or closed conformation (Table 2). Moreover, the distance separating the αIIb and β3 stalks of open molecules did not change when αIIbβ3 was bound to fibrinogen (13.4 ± 4.1 nm versus 12.6 ± 2.7 nm, respectively). The latter measurements suggest that stalk separation of approximately 13 nm is sufficient to identify active αIIbβ3 molecules. By contrast, in the presence of Mn^{2+}, there was an increase in both the length (10.9 ± 1.5 nm versus 12.6 ± 1.5 nm, $P < 10^{-8}$) and width (7.3 ± 1.5 nm versus 8.4 ± 1.1 nm, $P < 10^{-4}$) of the αIIbβ3 headpiece when αIIbβ3 shifted from a closed to an open conformation. In addition, the distance separating the stalks of open αIIbβ3 was significantly greater in the presence of Mn^{2+} than in the presence of Ca^{2+} (17.8 ± 3.6 nm versus 13.7 ± 4.1 nm, $P < 10^{-8}$). These measurements indicate that not only does Mn^{2+} shift αIIbβ3 from a closed to an open conformation by inducing the separation of αIIb and β3 stalks, but it also alters the overall size and shape of the headpiece.

Besides altering the size and configuration of individual αIIbβ3 molecules, Mn^{2+} increased their tendency to oligomerize. Whereas oligomers were uncommon in the presence of Ca^{2+}, 38% ± 10% of the open forms of αIIbβ3 in the presence of Mn^{2+} consisted of dimers, trimers, and higher-order oligomers (Figure 4A-C). Moreover, as shown in Figure 4D, the distribution of monomers, dimers, trimers, and higher-order oligomers could be fit to an exponential function (Figure 4D), as previously described for equilibria involving molecules that self-assemble into oligomers such as actin,[24,25]

Table 1. Analysis of transmission electron microscope images of purified αIIbβ3 molecules in the absence and presence of Mn^{2+}

	Group 1: closed structures, %	Group 2: open structures, %	Group 3: globular structures, %
Without Mn^{2+}	51 ± 12	11 ± 4	38 ± 10
With Mn^{2+}	24 ± 3	60 ± 4	17 ± 3

All the differences are statistically significant at *P* less than .001.

Table 2. Molecular dimensions of individual αIIbβ3 molecules in the presence of Ca^{2+} or Mn^{2+}

	No. of images measured	Head		Stalk separation, nm*
		Transverse length, nm*	Vertical length, nm*	
Ca^{2+}				
Closed	123	11.2 ± 1.5	8.0 ± 1.5	—
Open	97	12.1 ± 1.8	8.0 ± 1.6	13.7 ± 4.1
+ Fibrinogen	66	—	—	12.6 ± 2.7
Mn^{2+}				
Closed	95	10.9 ± 1.5	7.3 ± 1.5	—
Open	95	12.6 ± 1.5†	8.4 ± 1.1‡	17.8 ± 3.6
+ Fibrinogen	71	—	—	19.9 ± 4.7§

— indicates unmeasurable parameters.
*Data are given as mean ± 1 SD.
†Mn^{2+}/open versus Mn^{2+}/closed, $P < 10^{-8}$.
‡Mn^{2+}/open versus Mn^{2+}/closed, $P < 10^{-4}$.
§Mn^{2+}/fibrinogen versus Mn^{2+}/open, $P = 10^{-3}$.

hemoglobin S,[26] and prions.[27] It is also noteworthy that the oligomers resulted from interactions that exclusively involved the distal ends of the stalks and that oligomers composed of 3 or 5 molecules did not form closed rosettes as one would expect if the stalks underwent homomeric interactions.

Mn^{2+}-induced complex formation between αIIbβ3 and fibrinogen

Previously, we observed that αIIbβ3 bound to fibrinogen tended to have an open conformation with separated stalks.[23] To quantify these observations and to measure the distance separating the stalks when αIIbβ3 was bound to fibrinogen, we incubated fibrinogen with αIIbβ3 in the presence of 1 mM Mn^{2+} at 37°C for 30 minutes before the mixture was sprayed onto mica and rotary-shadowed with tungsten. As illustrated by Figure 5A, fibrinogen displayed its typical trinodular structure with 2 lateral D nodules and a central E nodule, and αIIbβ3 complexes were present in the 3 different conformations described in the previous section. Although the majority of individual fibrinogen and αIIbβ3 molecules were separated from each other, a minor fraction formed bimolecular and trimolecular complexes of 2 possible stoichiometric ratios, either 1:1 or 1:2 of αIIbβ3 to fibrinogen (Figure 5B-D). As we reported previously,[23] αIIbβ3 was always spatially oriented so that its headpiece was attached to the end of a fibrinogen molecule, and the stalks of 2 integrins attached to 1 fibrinogen were oriented in opposite directions. The orientation was such that the entire complex had a 2-fold axis of symmetry through the center of the fibrinogen, ie, a rotation of 180° about this axis brings one αIIbβ3 into the other one. All of the αIIbβ3 molecules interacting with fibrinogen were in the open conformation, implying that this conformation represents its activated state.

Because αIIbβ3 was in excess, quantitative analysis of complex formation was based on the relative proportion of fibrinogen molecules participating in the complexes versus those remaining free. Comparison of the fractions of free fibrinogen molecules in the presence and in the absence of Mn^{2+} clearly showed the promoting effect of manganese ions on fibrinogen binding to αIIbβ3. Thus, in the absence of Mn^{2+}, 23% ± 8% of the fibrinogen molecules were bound to αIIbβ3. In the presence of Mn^{2+}, the percentage increased significantly to 66% ± 6%. Further, we found that the distance separating the stalks of open αIIbβ3 increased from 17.8 ± 3.6 nm in the presence of Mn^{2+} alone to 19.9 ± 4.7 nm ($P = 10^{-3}$) when Mn^{2+}-treated αIIbβ3 was bound to fibrinogen (Table 2).

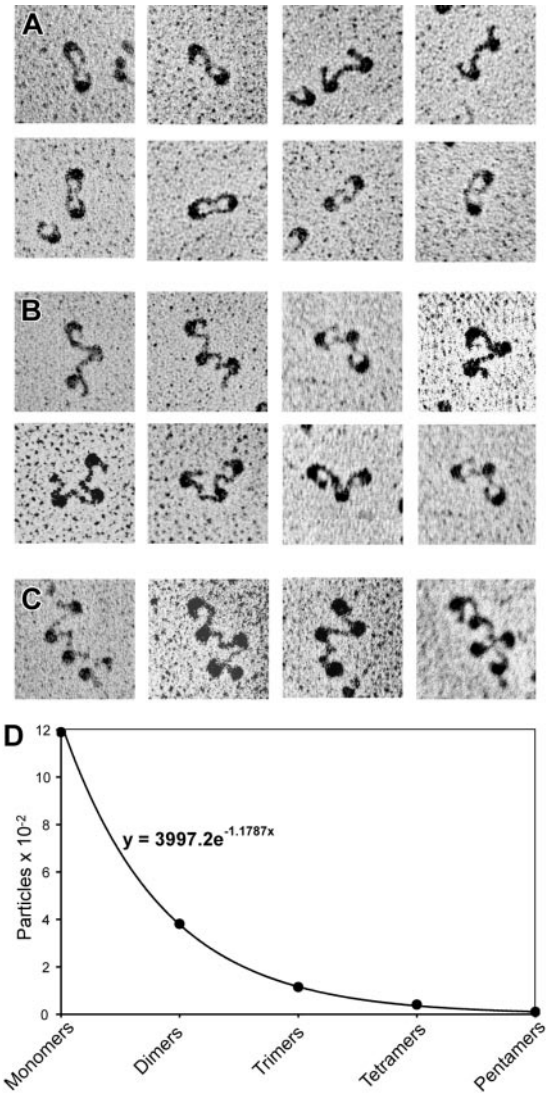

Figure 4. Transmission electron microscopy of αIIbβ3 oligomers observed in the presence of Mn^{2+}. (A) Most frequently, dimers were observed with 1-tail or 2-tail touching. (B) There were fewer integrin trimers. (C) Tetramers and larger oligomers were rare. (D) Size distribution of αIIbβ3 oligomers. These data were fit to an exponential function using Microsoft Excel. (A-C) Magnification, × 170 000.

DTT-induced changes in the activity and conformation of αIIbβ3

αIIbβ3 on platelets and transfected tissue culture cells is activated by incubating the cells with DTT.[5,6,28] Therefore, to determine

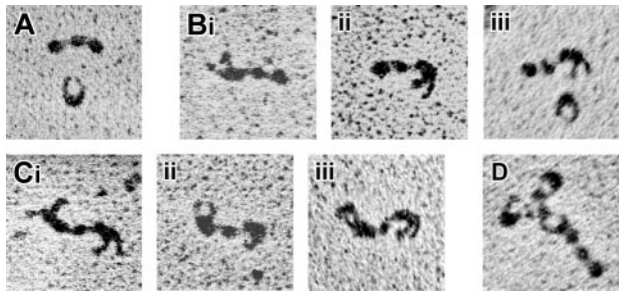

Figure 5. Transmission electron microscopy of αIIbβ3-fibrinogen complexes formed in the presence of Mn^{2+}. (A) Separate αIIbβ3 and fibrinogen molecules. (B-C) Bimolecular and trimolecular complexes of αIIbβ3 and fibrinogen. It is noteworthy that the αIIbβ3 molecules involved in these complexes all were in the open conformation. (D) Fibrinogen bound to an αIIbβ3 oligomer. Magnification, × 170 000.

whether the changes in the conformation of αIIbβ3 induced by Mn^{2+} are unique to this cation, we repeated the measurements described in the previous section using DTT as the stimulus for αIIbβ3 activation. First, we used laser tweezers to measure rupture forces between fibrinogen-coated beads and purified αIIbβ3 that had been preincubated with 5 mM DTT for 30 minutes in the presence of 1 mM Ca^{2+}. Similar to Mn^{2+}, DTT increased the cumulative probability of detecting rupture forces greater than 60 pN in the presence of Ca^{2+} from 1.9% ± 0.5% to 3.2% ± 0.6% (Table 3). Moreover, there was no difference between the average yield strength of fibrinogen binding to αIIbβ3 in the presence of Mn^{2+} or DTT, suggesting that the αIIbβ3 activation state was similar under both sets of conditions.

DTT-treated αIIbβ3 molecules were then visualized by transmission electron microscopy after rotary shadowing with tungsten. Like Mn^{2+}, DTT treatment resulted in a nearly 3-fold increase in the number of αIIbβ3 molecules in the open, rather than closed, conformation and in the formation of αIIbβ3 clusters. Further, DTT induced changes in the molecular dimensions of individual αIIbβ3 molecules that were similar to the changes induced by Mn^{2+}. Thus, the distance separating the αIIb and β3 stalks of open molecules significantly increased from 13.1 ± 2.8 nm in the presence of Ca^{2+} to 18.1 ± 3.9 nm in the presence of DTT and Ca^{2+} ($P = 4.8 \times 10^{-23}$) (Table 4). Moreover, there were significant increases in both the head length (11.9 ± 1.9 nm versus 13.4 ± 2.0 nm, $P < 10^{-6}$) and width (8.7 ± 1.4 nm versus 9.2 ± 1.1 nm, $P < .034$) when αIIbβ3 was treated with DTT. Thus, these measurements confirm that agents that activate αIIbβ3 by perturbing its extracellular domain induce separation of the αIIb and β3 stalks. They also indicate that these agents can alter the overall size and shape of the αIIbβ3 headpiece as well.

Table 4. Molecular dimensions of individual αIIbβ3 molecules in the presence of Ca^{2+} or DTT

	No. of images measured	Head		Stalk separation, nm*
		Transverse length, nm*	Vertical length, nm*	
Ca^{2+}				
Closed	96	11.6 ± 1.8†	9.0 ± 1.5‡	—
Open	93	11.9 ± 1.9§	8.7 ± 1.4‖	13.1 ± 2.8¶
DTT				
Closed	110	12.4 ± 1.5†	8.7 ± 1.2‡	—
Open	123	13.4 ± 2.0§	9.2 ± 1.1‖	18.1 ± 3.9¶

— indicates unmeasurable parameters.
*Data are given as mean ± 1 SD.
†Ca^{2+}/closed versus DTT/closed, $P = .027974$.
‡Ca^{2+}/closed versus DTT/closed, $P = .344849$.
§Ca^{2+}/open versus DTT/open, $P = 2.98 \times 10^{-7}$.
‖Ca^{2+}/open versus DTT/open, $P = 0.033581$.
¶Ca^{2+}/open versus DTT/open, $P = 4.85 \times 10^{-23}$.

Discussion

Integrins can be activated in vitro by cleavage with specific proteases,[29] stabilization of their activated states using monoclonal antibodies,[30] exposure to reducing agents such as DTT,[28] and incubation with the divalent cation Mn^{2+}.[31] How each of these treatments alters integrin activation states is not entirely clear. For example, although Ca^{2+} or Mg^{2+} are required for ligand binding to integrins, neither by themselves activate integrins, whereas Mn^{2+}, at millimolar concentrations, induces integrin-mediated cell adhesion,[4,9,31,32] binding of isolated integrins to immobilized ligands,[12,33,34] and binding of soluble ligands to integrins on cell surfaces.[35-37]

The crystal structure of the extracellular portion of the integrin αvβ3 revealed that it contains 8 divalent cation-binding sites.[14] Four sites were located in the β-propeller domain of αv, 1 at the α subunit genu (knee), and 3 in the β3 βA domain.[38] The number of divalent cations bound to the βA domain appears to be directly related to the presence or absence of ligand. Thus, in the absence of ligand, only the cation binding site in the βA ADMIDAS (adjacent to the metal ion-dependent adhesion site) motif is occupied,[14] whereas in the presence of Mn^{2+} and a cyclic Arg-Gly-Asp (RGD) ligand, each of the remaining 2 βA domain binding sites contain a cation. One of these sites is located in the βA MIDAS (metal ion-dependent adhesion site), and Mn^{2+} at this site contacts one of the ligand Asp carboxylate oxygens. A second Mn^{2+} is located 0.6 nm away from the MIDAS at a site designated as the ligand-induced metal binding site (LIMBS), but does not interact with ligand. Although it has been postulated that Mn^{2+} affects integrin activation states by antagonizing inhibitory effects of Ca^{2+},[9] analysis of the crystal structure of the αvβ3 extracellular domain suggests that by occupying sites in the MIDAS and LIMBS motifs of the βA domain, Mn^{2+} stabilizes its ligand-occupied conformation.[14]

Table 3. Comparison of Mn^{2+}- and DTT-induced fibrinogen binding to αIIbβ3 measured using laser tweezers

Conditions	Average yield strength, pN	Cumulative probability, %
Ca^{2+}	82 ± 15	2.1 ± 0.6
Mn^{2+}	88 ± 14	4.5 ± 0.8
No DTT, Ca^{2+}	89 ± 9	1.9 ± 0.5
DTT, Ca^{2+}	88 ± 9	3.2 ± 0.6

It is currently thought that integrins such as αIIbβ3 reside on cell surfaces in a thermodynamic equilibrium between inactive and active conformations that can be perturbed by altering the relative position of an integrin α and β stalks.[13,34] An essential element of this hypothesis is that the equilibrium can also be perturbed by altering the conformation of the integrin extracellular domain. To test this premise, we used laser tweezers–based force spectroscopy and electron microscopy to correlate the functional and ultrastructural consequences of exposing the platelet integrin αIIbβ3 to either Mn^{2+} or DTT. Laser tweezers are an optical system in which external forces applied to a spherical particle trapped by a laser can be accurately measured because the angular deflection of the laser beam is directly proportional to the lateral force applied to the particle and are sensitive and accurate at the lower end of the force spectrum (0-150 pN).[39,40] Previously, we found that specific binding of fibrinogen to αIIbβ3 resulted in rupture forces ranging from 60 to 150 pN and an average yield strength of 80 to 100 pN.[18] Because the specific rupture forces occurred as a single well-defined peak, they likely represent the interaction of individual αIIbβ3 and fibrinogen molecules. Using living platelets and isolated αIIbβ3 molecules, we found that Mn^{2+} and DTT increased the affinity of αIIbβ3 for fibrinogen and that the rupture forces between fibrinogen and Mn^{2+}- or DTT-stimulated αIIbβ3 were essentially the same as those we measured previously using ADP- and thrombin-related activation peptide (TRAP)–stimulated platelets.[18] Thus, like physiologic platelet agonists, Mn^{2+} and DTT shift αIIbβ3 from an inactive to an active conformation and do so in the absence of αIIbβ3 clustering. However, unlike Mn^{2+}- and DTT-activated α4β1 that was found to have an affinity for vascular cell adhesion molecule-1 (VCAM-1) or a ligand peptide intermediate between its inactive and fully active state,[41-43] we detected only 2 αIIbβ3 activation states. Thus, we found essentially no difference

in the spectrum of rupture forces between fibrinogen and αIIbβ3 regardless whether we measured it in the presence of Ca^{2+}, Mn^{2+}, or DTT or whether platelets were stimulated with ADP or TRAP. One might conclude erroneously that there are intermediate activation states when large ensembles of αIIbβ3 molecules are studied because time-averaged mixtures of low- and high-affinity αIIbβ3 molecules are being measured. Moreover, because the activation of integrin by Mn^{2+} is presumably reversible,[12] it is reasonable to assume that there is an equilibrium between the closed and open forms that is shifted toward the open form by Mn^{2+}. Thus, it is not necessary to hypothesize an intermediate conformer since such a conformer can be attributed to the mixture of 2 forms of the integrin.

The possibility that there are only 2 αIIbβ3 activation states is supported by the electron microscope images of single αIIbβ3 molecules. Although we detected 3 basic αIIbβ3 structures: open, closed, and globular, it is likely that the latter 2 are related because a comparable fraction of each was converted to the open form by Mn^{2+} or DTT. Similar images were obtained in earlier electron microscope studies of αIIbβ3[23] and α5β1,[13,36] regardless of the molecular staining technique. These structures were present in the absence of Mn^{2+} or DTT, but each agent converted most of the αIIbβ3 molecules to the open form. In electron microscope images of negatively stained αvβ3, Takagi et al[13] observed inactive molecules that had a bent conformation, similar to the bent conformation of αvβ3 in crystals,[38] and that αvβ3 was both extended and active in the presence of Mn^{2+}. We did not observe bent forms of αIIbβ3, even though our αIIbβ3 preparations clearly contained inactive and active molecules. However, Takagi et al[13] studied recombinant αvβ3 molecules containing a carboxyl-terminal clasp, whereas we studied αIIbβ3 molecules isolated from platelets. Accordingly, our studies and those of Takagi et al[13] may not be comparable.

Takagi et al[13] also observed that the Stokes (hydrodynamic) radius of Mn^{2+}-treated αvβ3 in the absence of ligand was intermediate between that of αvβ3 in the presence of Ca^{2+} and that of αvβ3 complexed with an RGD-containing ligand. However, Mould et al[44] observed no gross differences in the conformation of the α5β1 headpiece in the presence of Ca^{2+} and Mn^{2+} by solution x-ray scattering, but their data were also consistent with an opening of the headpiece that involved an outward movement of the β1 hybrid domain and downward swing of the α7 helix in the presence of Mn^{2+}. We did not detect a difference in the dimensions of the closed and open conformations of αIIbβ3 or in the distance separating the αIIb and β3 stalks of open and fibrinogen-bound αIIbβ3 in the presence of Ca^{2+}. Thus, these dimensions are at least sufficient to identify an active conformation of αIIbβ3. Moreover, like Takagi et al,[13] we found an increase in the size of the αIIbβ3 headpiece and a further increase in the distance separating the αIIb and β3 stalks in the presence of Mn^{2+} and DTT. Nonetheless, x-ray crystallography revealed no changes in the structure of the extracellular portion of αvβ3 when the crystals were soaked with buffer containing $MnCl_2$.[14] There are at least 2 possibilities to reconcile the difference between these results. First, contact forces in preexisting crystals may prevent the structural change normally induced by Mn^{2+}. Second, transmembrane and cytoplasmic segments absent in the crystal of the ectodomain may be critical to integrin activation because they were shown to have a major impact on the ligand-binding activity and the shape of the integrin.[45]

We found a clear correlation between the ability of αIIbβ3 to bind fibrinogen and the presence of open αIIbβ3 molecules. Thus, all αIIbβ3 molecules bound to fibrinogen, whether in the presence of Ca^{2+} or Mn^{2+}, had separated stalks. Moreover, we found that fibrinogen binding to αIIbβ3 was enhanced by Mn^{2+} and DTT in parallel with the increased fraction of open αIIbβ3 conformers. Because there is an equilibrium involving the inactive and active conformations of αIIbβ3, these observations suggest that the differential effects of Ca^{2+} and Mn^{2+} on the αIIbβ3 activation state are a function of the ability of each cation to stabilize one conformational state or the other. In the presence of Ca^{2+}, the probability of encountering an active open αIIbβ3 conformation was approximately 10%, but, in the presence of Mn^{2+}, the probability increased to approximately 60%. It is also noteworthy that, as would be expected in a chemical equilibrium, active and inactive molecules coexisted in the presence of either cation. Thus, Mn^{2+} appears to induce αIIbβ3 activity by stabilizing the active conformation of the αIIbβ3 headpiece, thereby shifting the chemical equilibrium in the active direction and transmitting the conformational change to the stalks. The changes in the dimensions of the αIIbβ3 headpiece are likely a consequence of the differences in size and electronegativity of Ca^{2+} and Mn^{2+} ions and of the additional Mn^{2+} bound to the headpiece in the presence of ligand.

Although αIIbβ3 activation by DTT likely involves overall disulfide bond reduction, as well disulfide bond rearrangement,[16] the identity of the cysteines involved is not clear. Because αIIbβ3 activation appears to involve changes in the conformation of βA and hybrid domains,[44,46-47] it would be logical to assume that the relevant cysteines are located in these domains, an assumption consistent with the changes in the dimensions of the αIIbβ3 headpiece that we detect in the presence of DTT. Nonetheless, the free cysteines identified when αIIbβ3 is exposed to mild reducing conditions are located in the epidermal growth factor-like repeats that constitute the β3 stalk,[16,38] as is an activating Cys583→Tyr mutation.[17] Thus, it is likely that the perturbed disulfide bonds that are responsible for αIIbβ3 activation by DTT remain to be identified.

Clusters of αIIbβ3 molecules have been observed on the surface of thrombin-stimulated platelets,[48] and αIIbβ3 clustering has been induced in vitro as well.[49-51] Using Mn^{2+}-activated αIIbβ3 and electron microscopy, we observed that in the absence of membrane or cytoskeletal constraints, isolated αIIbβ3 formed dimers, trimers, and higher-order oligomers that involved the distal ends of αIIb and β3 stalks. Thus, these images indicate that directly perturbing the activation state of the αIIbβ3 extracellular domain also results in the formation of αIIbβ3 oligomers in the absence of ligand, as would be predicted from the equilibrium model of integrin regulation. It is also noteworthy that the trimers and pentamers were always open, as would be predicted if the ends of the stalks only undergo homo-oligomerization, ie, the formation of α-α or β-β subunit oligomers. Although it is possible that this observation could be the result of steric interference, it is consistent with the hypothesis that homomeric associations involving transmembrane domains are associated with integrin activation and clustering.[45] It also suggests that a component of Mn^{2+}-induced modulation of integrin function in cell membranes may result in increased integrin avidity arising from Mn^{2+}-induced aggregation or clustering of integrin molecules.

In conclusion, we used laser tweezers and electron microscopy to demonstrate a direct correlation between conformational changes in individual αIIbβ3 molecules and their ligand-binding activity. Using Mn^{2+} and DTT as activating tools, we found that separation of the αIIb and β3 stalks is an integral part of the mechanism leading to the exposure of the fibrinogen binding site in the αIIbβ3 ectodomain. Moreover, because the open conformation induced by Mn^{2+} and DTT occurred in the absence of ligand binding, it likely represents a primary activating event, perhaps mimicking the consequences of agonist-induced stimulation of αIIbβ3 in platelet membranes.

References

1. Shattil SJ, Kashiwagi H, Pampori N. Integrin signaling: the platelet paradigm. Blood. 1998;91: 2645-2657.
2. Bennett JS. Structural biology of glycoprotein IIb-IIIa. Trends Cardiovasc Med. 1996;6:31-37.
3. Shimaoka M, Takagi J, Springer TA. Conformational regulation of integrin structure and function. Annu Rev Biophys Biomol Struct. 2002;31:485-516.
4. Paul BZS, Vilaire G, Kunapuli SP, Bennett JS. Concurrent signaling from $G\alpha_q$- and $G\alpha_i$-coupled pathways is essential for agonist-induced αvβ3 activation on human platelets. J Thrombos Haemostas. 2003;1:814-820.
5. Macintyre DE, Gordon JL. Evidence for two populations of disulfide bonds in blood platelets. Biochem Soc Trans. 1974;2:873-875.
6. Zucker MB, Masiello NC. Platelet aggregation caused by dithiothreitol. Thromb Haemostas. 1984;51:119-124.
7. Peerschke EI. Stabilization of platelet-fibrinogen interactions: modulation by divalent cations. J Lab Clin Med. 1993;121:135-141.
8. Kirchhofer D, Gailit J, Ruoslahti E, Grzesiak J, Pierschbacher MD. Cation-dependent changes in the binding specificity of the platelet receptor GPIIb/IIIa. J Biol Chem. 1990;265:18525-18530.
9. Smith J, Piotrowicz R, Mathis D. A mechanism for divalent cation regulation of beta 3-integrins. J Biol Chem. 1994;267:960-967.
10. Suehiro K, Smith JW, Plow EF. The ligand recognition specificity of beta3 integrins. J Biol Chem. 1996;271:10365-10371.
11. Cierniewski CS, Byzova T, Papierak M, et al. Peptide ligands can bind to distinct sites in integrin alphaIIbbeta3 and elicit different functional responses. J Biol Chem. 1999;274:16923-16932.
12. Yan B, Hu DD, Knowles SK, Smith JW. Probing chemical and conformational differences in the resting and active conformers of platelet integrin alpha(IIb)beta(3). J Biol Chem. 2000;275:7249-7260.
13. Takagi J, Petre B, Walz T, Springer T. Global conformational rearrangements in integrin extracellular domains in outside-in and inside-out signaling. Cell. 2002;110:599-611.
14. Xiong JP, Stehle T, Zhang R, et al. Crystal structure of the extracellular segment of integrin alpha Vbeta3 in complex with an Arg-Gly-Asp ligand. Science. 2002;296:151-155.
15. Adair BD, Yeager M. Three-dimensional model of the human platelet integrin alpha IIbbeta 3 based on electron cryomicroscopy and x-ray crystallography. Proc Natl Acad Sci U S A. 2002;99:14059-14064.
16. Yan B, Smith JW. Mechanism of integrin activation by disulfide bond reduction. Biochemistry. 2001;40:8861-8867.
17. Chen P, Melchior C, Brons NH, Schlegel N, Caen J, Kieffer N. Probing conformational changes in the I-like domain and the cysteine-rich repeat of human beta 3 integrins following disulfide bond disruption by cysteine mutations: identification of cysteine 598 involved in alphaIIbbeta3 activation. J Biol Chem. 2001;276:38628-38635.
18. Litvinov RI, Shuman H, Bennett JS, Weisel JW. Binding strength and activation state of single fibrinogen-integrin pairs on living cells. Proc Natl Acad Sci U S A. 2002;99:7426-7431.
19. Fowler WE, Erickson HP. Trinodular structure of fibrinogen. Confirmation by both shadowing and negative stain electron microscopy. J Mol Biol. 1979;134:241-249.
20. Weisel JW, Stauffacher CV, Bullitt E, Cohen C. A model for fibrinogen: domains and sequence. Science. 1985;230:1388-1391.
21. Veklich YI, Gorkun OV, Medved LV, Nieuwenhuizen W, Weisel JW. Carboxyl-terminal portions of the alpha chains of fibrinogen and fibrin. Localization by electron microscopy and the effects of isolated alpha C fragments on polymerization. J Biol Chem. 1993;268:13577-13585.
22. Kouns WC, Hadvary P, Haering P, Steiner B. Conformational modulation of purified glycoprotein (GP) IIb-IIIa allows proteolytic generation of active fragments from either active or inactive GPIIb-IIIa. J Biol Chem. 1992;267:18844-18851.
23. Weisel JW, Nagaswami C, Vilaire G, Bennett JS. Examination of the platelet membrane glycoprotein IIb/IIIa complex and its interaction with fibrinogen and other ligands by electron microscopy. J Biol Chem. 1992;267:16637-16643.
24. Zaner KS. Physics of actin networks. I. Rheology of semi-dilute F-actin. Biophys J. 1995;68:1019-1026.
25. Tuszynski JA, Brown JA, Sept D. Models of the collective behavior of proteins in cells: tubulin, actin, and motor proteins. J Biol Phys. 2003;29: 401-428.
26. Briehl RW, Mann ES, Josephs R. Length distributions of hemoglobin S fibers. J Mol Biol. 1990; 211:693-698.
27. Masel J, Jansen VA. The kinetics of proteinase K digestion of linear prion polymers. Proc R Soc Lond B Biol Sci. 1999;266:1927-1931.
28. Basani RB, D'Andrea G, Mitra N, et al. RGD-containing peptides inhibit fibrinogen binding to platelet alpha(IIb)beta3 by inducing an allosteric change in the amino-terminal portion of alpha(IIb). J Biol Chem. 2001;276:13975-13981.
29. Niewiarowski S, Kornecki E, Hershock D, et al. Aggregation of chymotrypsin-treated thrombasthenic platelets is mediated by fibrinogen binding to glycoproteins IIb and IIIa. J Lab Clin Med. 1985;106:651-660.
30. Ginsberg MH, Lightsey A, Kunicki TJ, Kaufmann A, Marguerie G, Plow EF. Divalent cation regulation of the surface orientation of platelet membrane glycoprotein IIb. J Clin Invest. 1986;78: 1103-1111.
31. Masumoto A, Hemler ME. Mutation of putative divalent cation sites in the alpha 4 subunit of the integrin VLA-4: distinct effects on adhesion to CS1/fibronectin, VCAM-1, and invasin. J Cell Biol. 1993;123:245-253.
32. Helluin O, Chan C, Vilaire G, Mousa S, DeGrado WF, Bennett JS. The activation state of αvβ3 regulates platelet and lymphocyte adhesion to intact and thrombin-cleaved osteopontin. J Biol Chem. 2000;275:18337-18343.
33. Vallar L, Melchior C, Plancon S, et al. Divalent cations differentially regulate integrin α_{IIb} cytoplasmic tail binding to β_3 and to calcium- and integrin-binding protein. J Biol Chem. 1999;274: 17257-17266.
34. Kim M, Carman CV, Springer TA. Bidirectional transmembrane signaling by cytoplasmic domain separation in integrins. Science. 2003;301:1720-1725.
35. Honda S, Tomiyama Y, Pampori N, et al. Ligand binding to integrin alpha(v)beta(3) requires tyrosine 178 in the alpha(v) subunit. Blood. 2001; 97:175-182.
36. Takagi J, Strokovich K, Springer TA, Walz T. Structure of integrin alpha5beta1 in complex with fibronectin. EMBO J. 2003;22:4607-4615.
37. Buensuceso C, de Virgilio M, Shattil SJ. Detection of integrin alpha IIbbeta 3 clustering in living cells. J Biol Chem. 2003;278:15217-15224.
38. Xiong JP, Stehle T, Diefenbach B, et al. Crystal structure of the extracellular segment of integrin αVβ3. Science. 2001;294:339-345.
39. Visscher K, Block SM. Versatile optical traps with feedback control. Methods Enzymol. 1998;298: 460-489.
40. Weisel JW, Shuman H, Litvinov RI. Protein-protein unbinding induced by force: single-molecule studies. Curr Opin Struct Biol. 2003;13:227-235.
41. Masumoto A, Hemler ME. Multiple activation states of VLA-4. Mechanistic differences between adhesion to CS1/fibronectin and to vascular cell adhesion molecule-1. J Biol Chem. 1993;268: 228-234.
42. Chigaev A, Blenc AM, Braaten JV, et al. Real time analysis of the affinity regulation of alpha 4-integrin. The physiologically activated receptor is intermediate in affinity between resting and Mn(2+) or antibody activation. J Biol Chem. 2001;276: 48670-48678.
43. Chigaev A, Zwartz GJ, Buranda T, Edwards BS, Prossnitz ER, Sklar LA. Conformational regulation of the alpha 4beta 1-integrin affinity by reducing agents: "inside-out" signaling is independent and additive to reduction-regulated integrin activation. J Biol Chem. 2004;279:32435-32443.
44. Mould AP, Symonds EJ, Buckley PA, et al. Structure of an integrin-ligand complex deduced from solution x-ray scattering and site-directed mutagenesis. J Biol Chem. 2003;278:39993-39999.
45. Li R, Mitra N, Gratkowski H, et al. Activation of integrin alphaIIbbeta3 by modulation of transmembrane helix associations. Science. 2003; 300:795-798.
46. Mould AP, Barton SJ, Askari JA, et al. Conformational changes in the integrin beta A domain provide a mechanism for signal transduction via hybrid domain movement. J Biol Chem. 2003;278: 17028-17035.
47. Yang W, Shimaoka M, Chen J, Springer TA. Activation of integrin beta-subunit I-like domains by one-turn C-terminal alpha-helix deletions. Proc Natl Acad Sci U S A. 2004;101:2333-2338.
48. Fox JE, Shattil SJ, Kinlough-Rathbone RL, Richardson M, Packham MA, Sanan DA. The platelet cytoskeleton stabilizes the interaction between $\alpha_{IIb}\beta_3$ and its ligand and induces selective movements of ligand- occupied integrin. J Biol Chem. 1996;271:7004-7011.
49. Hato T, Pampori N, Shattil SJ. Complementary roles for receptor clustering and conformational change in the adhesive and signaling functions of integrin $\alpha_{IIb}\beta_3$. J Cell Biol. 1998;141:1685-1695.
50. Hantgan RR, Paumi C, Rocco M, Weisel JW. Effects of ligand-mimetic peptides Arg-Gly-Asp-X (X = Phe, Trp, Ser) on αIIbβ3 integrin conformation and oligomerization. Biochemistry. 1999;38: 14461-14474.
51. Hantgan RR, Lyles DS, Mallett TC, Rocco M, Nagaswami C, Weisel JW. Ligand binding promotes the entropy-driven oligomerization of integrin αIIbβ3. J Biol Chem. 2003;278:3417-3426.